Effects of Environmental Flow upon Tropical Cyclone Structure

WILLIAM M. FRANK AND ELIZABETH A. RITCHIE*

Department of Meteorology, The Pennsylvania State University, University Park, Pennsylvania

(Manuscript received 9 February 1998, in final form 27 July 1998)

ABSTRACT

Numerical simulations of tropical-cyclone-like vortices are performed to analyze the effects of unidirectional vertical wind shear and translational flow upon the organization of convection within a hurricane's core region and upon the intensity of the storm. A series of dry and moist simulations is performed using the Pennsylvania State University–National Center for Atmospheric Research Mesoscale Model version 5 (MM5) with idealized initial conditions. The dry simulations are designed to determine the patterns of forced ascent that occur as the vortex responds to imposed vertical wind shear and translational flow, and the mechanisms that modulate the vertical velocity field are explored. The moist simulations are initialized with the same initial conditions as the dry runs but with a cumulus parameterization and explicit moisture scheme activated. The moist simulations are compared to the dry runs in order to test the hypothesis that the forced vertical circulation modes modulate the convection and hence latent heat release in the hurricane core, as well as to evaluate the net effect of the imposed environmental flow on the storm intensity and structure.

The results indicate that the pattern of convection in the storm's core is strongly influenced by vertical wind shear, and to comparable degree by boundary layer friction. In the early stages of moist simulations, typical of the tropical depression stage, the regions of forced ascent and the mechanisms that cause them are similar to those in the dry runs. However, once the moist storm runs deepen enough to develop saturation in part of the eyewall, the patterns of vertical motion and associated rainfall differ between the paired dry and moist runs with identical initial conditions. The dry runs tend to produce a strong, deep region of ascent in the sector of the storm that lies downshear right of the center. The moist runs begin similarly, but as the storms intensify they strongly favor upward motion and rainfall downshear left of the center.

It appears that the vertical motion patterns in the dry and moist simulations are dominated by similar adiabatic lifting mechanisms prior to the development of partial eyewall saturation. Once the moist runs reach saturation, this adiabatic lifting mechanism no longer occurs due to the latent heat release within the ascending air. Hence, the patterns of forced ascent in the dry runs should be relevant for understanding patterns of convection in loosely organized systems such as tropical depressions, but not in mature hurricanes. The rainfall patterns produced by the moist simulations are in good agreement with recent observational analyses of the relationships between rainfall distribution and vertical wind shear in Atlantic hurricanes.

1. Introduction

a. Overview

Tropical cyclones are remarkably intense and stable vortices. They frequently exhibit lifetimes of 2 weeks or more, and they rarely dissipate over tropical waters. Nevertheless, their robust nature does not imply that these storms are impervious to external influences. The storms frequently undergo major changes in structure during their lifetimes. These structural variations cause major variations in the distribution and intensity of wind and rain, and through interactions with the ocean surface they also have large effects upon waves and storm surge. While some fluctuations in core structure are probably due to internally generated wave processes, there is increasing evidence that many structural variations in cyclones are caused by interactions between the storm and its environment. Therefore, much of the variability in tropical cyclone structure and intensity should be predictable from knowledge of the storm's environment.

Previous research has revealed that even moderate changes in the magnitude or vertical shear of the mean winds can alter the storm in ways that could potentially affect the structure and intensity of the cyclone, as well as its path (e.g., Jones 1995; DeMaria 1996; Bender 1997). The current paper examines the basic question of how the mean zonal winds and the vertical shear of these winds affect storm structure. The major emphasis is upon the manner in which the zonal winds and bound-

* Current affiliation: Department of Meteorology, U.S. Naval Postgraduate School, Monterey, California.

Corresponding author address: William M. Frank, Department of Meteorology, The Pennsylvania State University, University Park, PA 16802.
E-mail: frank@ems.psu.edu

ary layer processes modulate the vertical velocity field within the storm. It is hypothesized that these processes dynamically force regions of ascent and descent within the cyclone, and that they thereby organize and control the amount and distribution of latent heat release. This process should have significant effects upon the structure and intensity of the system.

Although tropical cyclones have been studied intensively throughout the twentieth century, we have surprisingly little quantitative knowledge as to how the storms interact with their environments, particularly with respect to changes in core structure. (Storm motion, while hardly a solved problem, is much better understood.) The major problems that inhibit progress in this area are the chronically sparse data over the tropical oceans and the difficulties in separating cause and effect in complex systems with important, interacting processes occurring on several scales. Numerical simulation provides a viable alternative to observations for the purpose of analyzing tropical cyclone–environmental interactions. While models are subject to a great many limitations of their own, they nonetheless allow the researcher to isolate and control both features of the large-scale environment of the storm and some of its internal processes.

This paper presents results of a series of numerical simulations designed to study effects of imposed external circulation features upon the structure of tropical-cyclone-like vortices. The current paper examines the first-order effects of mean zonal flow, including vertical shear, and of surface friction upon the structure of an initially balanced baroclinic vortex that resembles a tropical depression. Future work will address interactions between tropical cyclones and more complex external circulations.

b. Background

The structure and evolution of tropical cyclones was reviewed by Willoughby (1995). The primary energetic principles of these storms are thought to be well understood. They extract significantly above-normal amounts of latent and sensible heat from the sea surface due to the intense winds in the core region. The latent heat is released as air ascends to the upper troposphere in the eyewall cloud and other rainbands that contain deep convective cores, and this heating warms the core to virtual temperatures close to those of a moist pseudoadiabat for boundary layer air. The air diverges in the upper levels and gradually descends on larger scales as it cools radiatively. The storm's energetics have been compared to a Carnot-cycle steam engine by Emanuel (1986). During the intensification stage of the life cycle, the strong diabatic heating in the eyewall region leads to contraction of the core, which in turn spins up the winds (e.g., Shapiro and Willoughby 1982). In a mature, approximately steady-state tropical cyclone there is a balance in the core's kinetic energy cycle between the frictional dissipation in the boundary layer and its generation by downgradient inflow (Frank 1977).

Given the dominant role of latent heat release in tropical cyclone energetics, it is not surprising that most hypotheses on the causes of storm structure and intensity change relate in some way to processes that affect amounts and distributions of latent heat release. Most research in this area has focused on processes that affect the total supply of moisture to the storm or the maximum values of equivalent potential temperature that may be achieved in the boundary layer. There has been some success in relating sea surface temperatures (SST) beneath the core to cyclone intensity (DeMaria and Kaplan 1994), and there have been cases where dry advection in the middle troposphere has been suggested as a cause of storm weakening. Thermodynamic arguments suggest an upper limit to the maximum intensity of a tropical cyclone that is proportional to the SST and some measure of the depth of the convection, such as the height of the tropopause (Emanuel 1988, 1997; Holland 1997). Applications of this concept to intensity forecasts of individual storms has met with limited success, apparently due to the fact that few storms reach their maximum potential intensity (e.g., Lighthill et al. 1994). However, the thermodynamic controls on the total latent heat release are only part of the story.

Other recent studies have found that both the total amount of convection and the storm intensity (defined either in terms of the minimum sea level pressure or the maximum wind speed) appear to be strongly affected by interactions between the storm and external circulations. For example, case studies by Molinari et al. (1995) and others have shown that upper-level potential vorticity (PV) anomalies, such as those associated with upper-level troughs, can weaken a tropical cyclone by increasing vertical shear over the core, or intensify it either by unbalancing the upper-level flow leading to enhanced divergence of mass from the core (hence increasing the total convection) or as a result of superposition of the upper- and lower-level PV anomalies. Modeling studies such as Pfeffer and Challa (1992) support the positive influence of enhanced upper-level outflow on storm intensification.

While the organization of moist convection usually defies simplistic explanations, it appears to be universally true that it is heavily modulated by circulations that cause dynamically forced regions of vertical motion. The secondary circulations that result in regions of ascending and descending motion within tropical cyclones have been ascribed to several mechanisms. Part of a tropical cyclone's inflow results from direct response to the latent heat release in the core, which causes a thermally direct secondary circulation (Willoughby 1995). The mean, axisymmetric inflow resulting from this process tends to be relatively weak (less than 1 m s^{-1}), but it occurs through a deep layer, typically extending from the surface up to about 300 hPa. Within the rainbands themselves, the latent heating produces

such a strong positive feedback on the local upward motion that it is difficult to ascribe the underlying causes of the preferred regions of ascent. There are several theories relating the organization of tropical cyclone rainbands to various wave types, as reviewed by Willoughby (1995), but this paper will not directly address that problem. Rather, it will seek to examine and compare the relative effects of vertical shear and boundary layer processes upon the vertical velocity field in the core region and how they thereby modulate the storm's convection and intensity.

As shown by many studies, the typical tropical cyclone has a distinct inflow layer extending from the sea surface to a height of about 2 km, with the strongest inflow occurring near the surface. The top of this layer appears to be roughly constant over a large area, but it decreases to sea level near the eyewall (Frank 1982, 1984). Most sources attribute the majority of this inflow to the effects of friction, though aircraft measurements of stress typically have not noted large values of stress above about 500–600 m (e.g., Moss and Merceret 1976; Frank 1984). Because boundary layer stress varies quadratically with wind speed, it produces a band of convergence near the radius of maximum winds, hence at or near the eyewall (Willoughby 1995). Depending upon the radial profile of the rotational winds in a particular storm, boundary layer friction may also cause bands of low-level convergence outside the eyewall. Shapiro (1983) used a simple slab boundary layer model to analyze the effects of storm movement on the pattern of frictional convergence. He found that for slow-moving storms the convergence was concentrated in the right front quadrant (looking downstream), while for faster-moving storms it was located more directly in front of the center.

Several observational studies of Atlantic hurricanes have shown that patterns of convection in the eyewall region tend to exhibit persistent asymmetries that appear to be related to the asymmetric wind field in or near the center of the storms (Willoughby et al. 1984; Marks et al. 1992; Franklin et al. 1993). In particular, each of the case studies described in these papers suggests that the precipitation in hurricanes tends to be maximum on the left side of the vertical shear vector (looking downshear).

The manner in which vertical shear modulates the secondary circulations of tropical cyclones and produces asymmetries has been explored in recent modeling studies by Shapiro (1992), Jones (1995), DeMaria (1996), and Bender (1997). Vertical wind shear has long been known to be unfavorable for tropical cyclogenesis, and strong shear also tends to favor weakening of mature cyclones (Gray 1968; Merrill 1988). Early studies focused on the possible role of the shear in advecting the warm, moist air out of the core, but more recent analyses have tended to focus on its dynamic effects on the structure of the core.

Shapiro (1992) used a three-layer model to examine the effects of westerly shear in the upper troposphere upon the motion of a hurricane-like vortex on an f-plane. He found that the vortex drifted slowly to the southeast due to the interactions between the vortex and the negative meridional PV gradient in the middle layer of his model that was associated with the imposed vertical shear.

Jones (1995) used a primitive equation model to study the effects of vertical shear upon the motion and structure of dry, frictionless, barotropic vortices on an f-plane. She imposed linear shear profiles and found that as the shear tilted the initially balanced vortex, the flow responded in a manner that kept the flow close to a balanced state. Upper- and lower-level vorticity centers tended to rotate around each other, and the vortex developed a secondary circulation pattern with a wavenumber one structure. This vertical circulation pattern resulted from an isentropic flow mechanism that is discussed later. Jones also explored the effects of variations in vortex structure and of several environmental properties (shear strength, static stability, and Coriolis parameter) upon her results.

DeMaria (1996) examined the effects of vertical shear on tropical cyclone intensity change using a two-layer model. His results suggested that the negative influence of shear on cyclone intensity results not from ventilation of the core, as had been suggested in earlier studies, but from inhibition of convection due to midlevel warming and hence stabilization associated with the balanced response to tilt of the vortex by the shear. He noted that larger, stronger, and higher-latitude storms are less sensitive to shear than are their counterparts.

Bender (1997) simulated the effects of mean flow, vertical shear, friction, and variable f (Coriolis parameter) on hurricane structure using the full-physics Geophysical Fluid Dynamics Laboratory model. He analyzed patterns of convergence, vertical velocity, and rainfall in the model under the influence of various imposed mean flow conditions, and he examined the effects of relative flow on the relative vorticity field. For the range of conditions studied, Bender's (1997) simulations indicated that the β-gyres resulting from variable f tended to force low-level convergence and ascent on the rear side of the eyewall. Adding mean flow caused the upward motion to be concentrated in the left front quadrant, while vertical shear tended to cause uplifting on the downshear side. Rainfall patterns showed agreement with the regions of uplifting. All of the simulations involving mean flow were performed with the cumulus parameterization activated, making it somewhat difficult to isolate the nature and magnitudes of individual dynamical processes, but sensitivity of the model to variations in the mean flow were clearly established. Bender (1997) concluded that most of the asymmetries that occurred in his simulations resulted from changes in the direction and vertical shear of the storm-relative asymmetric winds in the core.

The current study has several aspects in common with

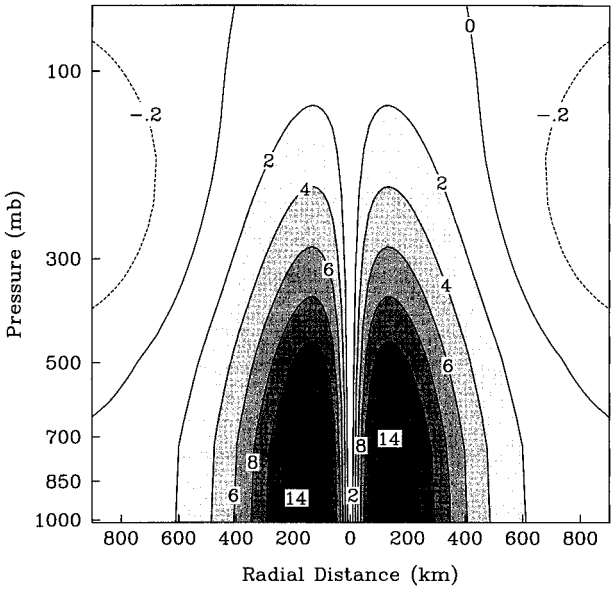

FIG. 1. Tangential winds for the initial balanced vortex (m s^{-1}). Only the fine mesh domain is shown.

Jones (1995) and Bender (1997), but it also has several major differences. This study combines a series of idealized simulations using a dry model followed by complementary runs with the moist parameterizations activated. In this way we hope to isolate the different physical processes contributing to the secondary circulation as well as their relative magnitudes and interactions. The methodology followed for the dry runs is similar to that of Jones (1995), but it differs in several important ways. This study uses a baroclinic (rather than barotropic) initial vortex, and it includes a high-resolution boundary layer model, so that the effects of boundary layer friction and vertical shear upon the secondary circulation can be compared and contrasted. In addition, the dry model runs are compared to simulations performed using parameterized moist convection to examine the effects of latent heat release upon the results. The primary differences in methodology from Bender (1997) are that the current study uses the paired dry and moist runs, a different numerical model (that includes, e.g., fully explicit moist processes in addition to parameterization), and analyzes the results in terms of balance arguments rather than budgets.

2. Methodology

a. Experimental design

The simulations described below show the behavior of an initial tropical-depression-like vortex (hereafter referred to as the TD vortex) in different environmental flows. The initial vortex (Fig. 1) resembles a strong tropical depression that is only slightly below the intensity threshold of 17 m s^{-1} winds used to classify the system as a tropical storm in the Atlantic basin. It is based on data from a composite analysis of a prestorm tropical depression by McBride and Zehr (1981). It is a warm-core system with maximum winds of 15 m s^{-1} at a radius of 135 km, and there is a weak upper-level anticyclone. This relatively weak stage of the cyclone was chosen because we did not want the relatively subtle circulations caused by the interactions between storm and environment to be obscured by the primary flow. For example, tropical depressions are almost always more asymmetric than fully developed hurricanes, and one area of interest is the development of asymmetries in the storm circulation.

TABLE 1. Model configuration for the cases shown in the first column shows whether or not the boundary layer scheme was activated. The third column indicates whether the domain mean zonal wind was zero or −3 m s^{-1} (easterly = E), and the fourth column shows the direction of the shear (0 = zero, W = westerly, E = easterly).

Case	PBL	Zonal flow	Shear
A1	No	0	0
A2	Yes	0	0
B	Yes	E	0
C1	No	0	E
C2	Yes	0	E
C3	Yes	E	E
D3	Yes	E	W
M (control)	Yes	0	0
MC2	Yes	0	E
MC3	Yes	E	E
MD2	Yes	0	W
MD3	Yes	E	W

The runs are performed with different mean values of the zonal wind, with different vertical shears of the mean zonal wind, and with the boundary layer scheme (and hence friction) turned on and off (Table 1). The resulting effects on vortex structure are analyzed, paying particular attention to changes in the following quantities: the central pressures and maximum winds of the TD vortex, indicating a tendency for the system to weaken or strengthen in response to environmental conditions; asymmetries in the core structure; and development of secondary circulations, especially regions of low-level or deep-layer convergence or divergence that would be expected to cause changes in the amount and distribution of moist convection within the core region.

Although diabatic heating, particularly latent heat release, is of fundamental importance to the energetics of tropical cyclones, many of the simulations performed here use a dry version of the model with no diabatic heating. This is done in order to isolate the relatively subtle but direct interactions between imposed environmental flow properties and the structure of the TD vortex. The goal is to examine first-order effects of these interactions. The results are then used to guide subsequent simulations using a relatively simple cumulus parameterization to examine the effects of latent heating upon the results. As noted above, ongoing and future research will extend this work to include finer mesh

simulations with explicitly resolved convection and to examine more complex external circulations.

b. Model description

The simulations are performed with the nonhydrostatic Pennsylvania State University–National Center for Atmospheric Research Mesoscale Model version 5 (MM5) (Anthes et al. 1987). This model incorporates multiple nested grids and includes both explicit moist physical processes and a variety of cumulus parameterization and boundary layer schemes. It solves the nonlinear, primitive equations using Cartesian coordinates in the horizontal and a terrain-following sigma coordinate in the vertical. The model has been adapted for use with idealized initial conditions to permit careful control of initial value experiments.

The use of a model of this type is crucial for accomplishing the long-term goals of the project. Numerical simulations of tropical cyclone–environmental interactions require a model with a very large domain, needed to resolve the storm's environment and external circulation features, as well as a high-resolution core region capable of resolving the small, intense core of the storm. While many of the simulations shown in this paper are made with a dry version of the model, only limited progress is possible without including the latent heating processes and their effects. Ideally, the model should attempt to resolve moist processes explicitly, at least in the core region, since the eyewall region of hurricanes has too intense and complex a structure to permit full resolution using cumulus parameterization techniques. However, first-order processes are often easier to diagnose using simpler models, and the moist runs shown in this paper are performed using parameterized cumulus convection working in combination with the explicit moisture scheme.

All simulations are performed on an f-plane valid at 15°N. Although use of a variable f would allow a more physically consistent comparison between the simulated hurricanes and real ones, it would also introduce complications in isolating directs effects of shear on the core. With a variable f the cyclone tends to develop β-gyre circulations due to interactions between the storm's primary circulation and any existing PV gradient. This changes the asymmetric flow in the core region, making it a function of both the large-scale flow imposed in the initial conditions and the interactions between the storm and the vorticity field. The changes in the core winds are significant and involve not only alterations of the asymmetric wind speed and direction but also the vertical shear. This induced flow often exhibits a jetlike structure with maximum winds occurring in the lower troposphere [see Figs. 4 and 14 of Bender (1997)]. Hence, the actual shear across the storm center could be quite different in strength, direction, and vertical mode from that proscribed in the initial conditions. The f-plane was chosen for these initial simulations to provide a more controlled environment for isolating cause and effect in the eyewall region, but future work will include variable f as well as other model changes designed to allow a closer comparison to real storms.

The model is configured with 20 vertical levels, 7 of which are below 850 hPa. The domain is square and is 5400 km on each side. The coarse mesh is 45 km, and there is a nested fine mesh region that is 1800 km on a side with 15-km resolution. Each mesh consists of 121 by 121 points. The boundary layer is parameterized using the Blackadar (1976, 1979) scheme, which was further described and tested by Zhang and Anthes (1982). The lower boundary is an ocean surface at a constant temperature of 28.5°C. For the moist simulations, a cumulus parameterization is used (Betts and Miller 1986). The explicit moisture scheme, which treats rainwater and cloud water as explicit variables, is also activated for the moist runs to deal with any grid-scale condensate. The initial winds are in gradient balance with the mass field. All simulations are performed with mean zonal flows of either zero or -3 m s^{-1} (easterly). Some have a zonal shear component added, as is discussed later. All simulations begin with the baroclinic vortex shown in Fig. 1 and described earlier. Relative humidity values are from the McBride and Zehr (1981) prestorm cluster composite with a positive anomaly added in the vortex core region to facilitate onset of convection.

3. Results

a. Dry model simulations

1) Zero environmental flow: Case A

Case A consisted of two simulations performed with the environmental winds set to zero everywhere. In experiment A1 the model was initialized with the balanced, symmetric vortex described above, and the boundary layer scheme was turned off to remove surface friction effects. The simulation was run for 48 h, and there were no apparent changes in vortex structure except for some very small wind changes due to diffusion. This run was made simply to demonstrate the stability of the initial vortex. Similar tests showed that the vortex also remained stable when mean zonal environmental flow was added. All simulations were performed using the same initial vortex unless otherwise noted.

The above simulation was rerun with the high-resolution boundary layer scheme activated (experiment A2). The primary effect of surface friction was to cause symmetric frictionally induced inflow in the boundary layer, which produced an axisymmetric band of convergence near and outward from the radius of maximum winds. The location of this convergence band agreed well with that predicted from simple balance theory in which it is assumed that the frictional dissipation of angular momentum is balanced by inward advection of angular momentum, following Willoughby (1995) and based on earlier work by Smith (1968).

It should be noted that in case A2 (and in all subsequent cases in which the boundary layer scheme was activated at the beginning of the simulation) shallow, outward-propagating gravity waves occurred. These resulted from the initial imbalance created when friction was added to the flow. These gravity waves were observed to propagate outward at about 3.5 m s^{-1}, and a cross-sectional analysis (not shown) revealed them to be largely confined to the lowest 2 km or so. This is almost exactly equal to the speed of a linearly propagating gravity wave with vertical wavelength of 2 km (equal to 3.2 m s^{-1} for the stability used in the model). These waves do not appear to have had any significant impact on the results discussed below.

The ascent near the radius of maximum winds was forced by boundary layer friction, and it decreased rapidly with height. At 950 hPa (near cloud base for a typical tropical depression) the maximum vertical velocities between 12 and 24 h were about 1.2 cm s^{-1}. At 700 hPa the maxima were of order 0.2 cm s^{-1}, and at 500 hPa they were very weak, a mere 0.1 cm s^{-1}. Hence, any organization of convection driven by the convergence in this case would have had to occur due to convergence in the lowest levels, primarily at or below cloud base.

The surface friction slowly reduced the wind speeds in the boundary layer, and without the positive feedbacks from latent heat release, the storm gradually weakened. Both vertical velocities and the cyclonic circulation gradually decreased after about 6 h. In real systems this spindown is offset by the latent heat release, but for dry runs the storm gradually evolved away from a structure that is typical of a tropical cyclone. Therefore, for dry runs with the boundary layer scheme activated, results are presented only for the first 24 h.

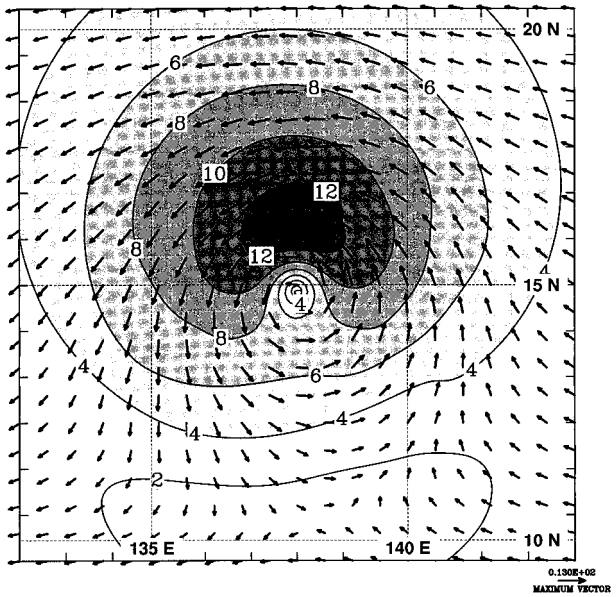

FIG. 2. Plan view of the winds at 950 hPa, $t = 24$ h, for case B (easterly zonal flow, no shear). Units are m s^{-1}, and the longest vector is 13 m s^{-1}. The figure shows a portion of the fine mesh grid area (1200 km on a side), with latitude–longitude lines added for reference.

2) EASTERLY FLOW, NO SHEAR: CASE B

In case B the vortex was initialized in a horizontally and vertically uniform mean easterly flow of 3 m s^{-1} with the boundary layer scheme activated. The 3 m s^{-1} flow is rather weak, but since dry simulations do not have the strong vertical mass fluxes that help to provide vertical coupling in a cyclone, we chose weak mean winds and vertical shears to maintain the structural integrity of the vortex as long as possible. Unlike the zero-flow case (A2) described above, the moving vortex began with and maintained a horizontal wavenumber one asymmetry in the low-level wind field. Figure 2 shows the winds at approximately 950 hPa at $t = 24$ h. The system had moved westward with the mean flow, with the maximum winds remaining on the right side of the center. This pattern was maintained vertically through most of the troposphere. There was no significant tendency for the low-level wind maximum to occur ahead of the storm center or in the right front quadrant as was found in a study of fully developed hurricanes by Shapiro (1983). This difference may have been due to the weaker and more slowly moving vortex used in the current study, but it also could have resulted from differences in the nature of the models used. We are investigating the causes of the differences.

The boundary layer friction combined with the movement of the storm caused a more complex pattern of low-level vertical velocity (Fig. 3) than was observed for the stationary storm. The 950-hPa w field at 24 h showed a concentration of upward motion in the right front quadrant and generally descending air in the left rear quadrant, in agreement with Shapiro (1983). The pattern was complicated by a series of bands, which again appeared to be shallow gravity waves. There was a slight tendency for the location of the maximum upward motion to rotate cyclonically during the simulation.

As was true for case A2, the vertical velocities were much weaker at 700 hPa than at 950 hPa, indicating the relatively shallow extent of the frictional effects. The dipole of vertical velocity, with upward motion in the right front–downward motion in the left rear quadrants, was clearer at 700 hPa.

3) EASTERLY SHEAR: CASE C

In cases C1 (frictionless) and C2 (boundary layer scheme activated) the vortex was embedded in mean easterly flow that varied from $u = 0$ near the surface to -3 m s^{-1} in the upper troposphere, with maximum shear near 500 hPa (Fig. 4). Case C3 was the same as C2 except an additional easterly mean flow of 3 m s^{-1} was added at all levels. In C1 the shear caused the vortex

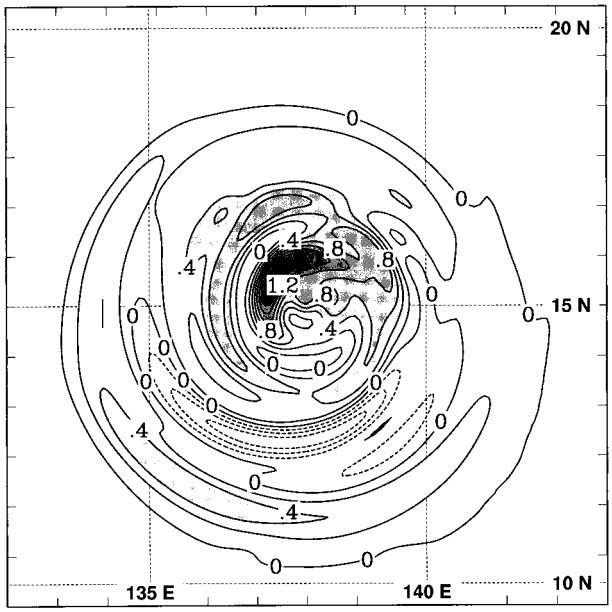

FIG. 3. Vertical velocity (cm s^{-1}) at 950 hPa, 24 h, for case B. The contour interval is 0.2, and positive values greater than 0.2 are shaded.

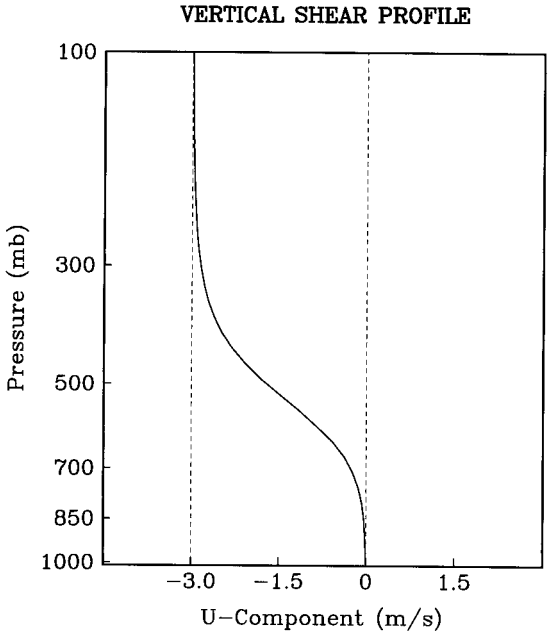

FIG. 4. The vertical variation of the zonal wind (m s^{-1}) used for the easterly shear cases.

to tilt downstream with time. The 6-hourly positions of the vortex center at four different levels are shown in Fig. 5 for a 48-h integration. The vorticity maximum at 500 hPa, near the center of mass of the column, moved slightly to the south of due westward, while the upper-level vortex center (200 hPa) moved almost directly westward with the mean flow. In both cases, they moved at the approximate velocity of the imposed winds at that level. However, the vortex centers just above the surface and at 700 hPa moved to the right of the mean flow (toward the northwest) following nearly linear tracks throughout the 48 h at speeds between 0.5 and 1.0 m s^{-1}. Comparing these latter motions to Fig. 4 it can be seen that the flow relative to the surface vortex is front to back (looking down the track), and the relative flow is generally back to front above about 700 hPa.

The simplest explanation for the component of northward movement of the lower portions of the vortex may be visualized by considering the tilt of the balanced vortex by the imposed shear. This process has been described by Jones (1995) and others and is applicable to the current case where the relatively weak flow tilts a vortex that is initially in gradient balance. Briefly, as the vortex begins to tilt downshear, the winds and mass field become unbalanced, and a compensating secondary circulation develops to restore the balance. The most convenient way to think of this process is in terms of the downward and upward reflections of PV centers at different levels as they advect downshear. Thus, as mid-level slabs of PV are advected downshear, they induce low-level convergence and increasing vorticity west of the low-level vortex center. The resulting flow is northward at the location of the low-level vortex, advecting it northward. The reverse effect occurs in the upper-middle troposphere. Jones (1995) found similar movements in her simulations of barotropic hurricane-like vortices, but in her results the vortex centers rotated around each other. In the present case the vortex centers shown near the surface and at 200 hPa moved with

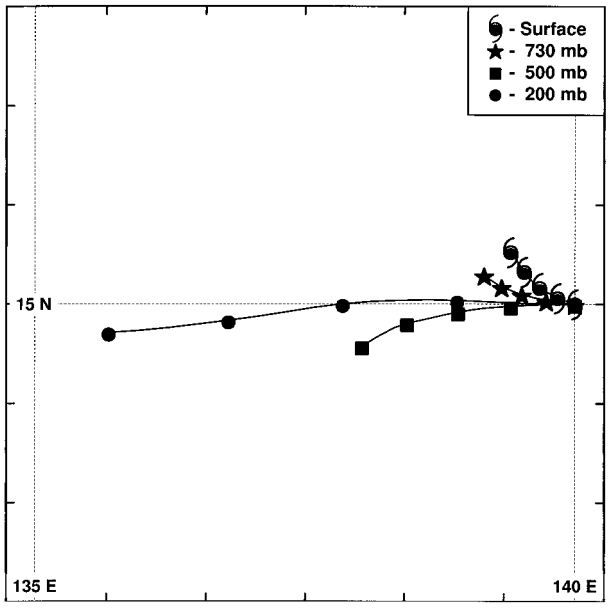

FIG. 5. Positions of the vorticity centers at four vertical levels and at 12-h intervals for case C1 (easterly shear, no zonal flow, no boundary layer).

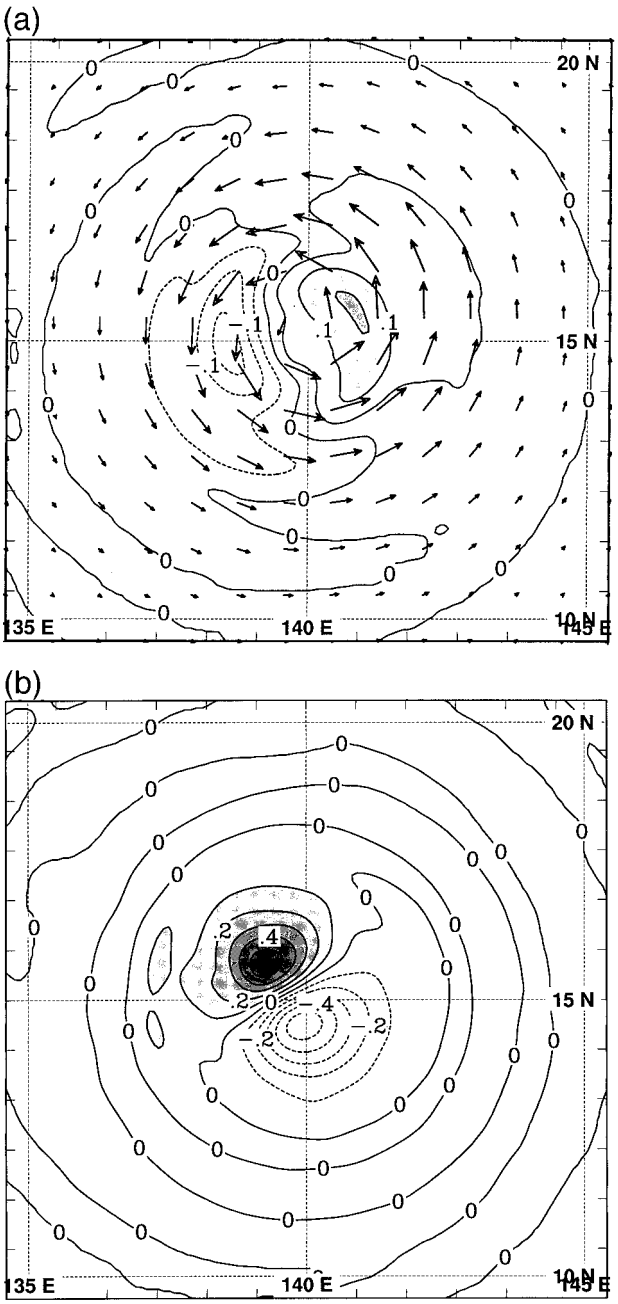

FIG. 6. (a) Wind barbs and potential temperature contours (K) at 950 hPa, 24 h, for case C1. (b) Vertical velocity (cm s^{-1}) at 950 hPa, 24 h, for case C1. The contour interval is 0.1, and positive values greater than 0.1 are shaded.

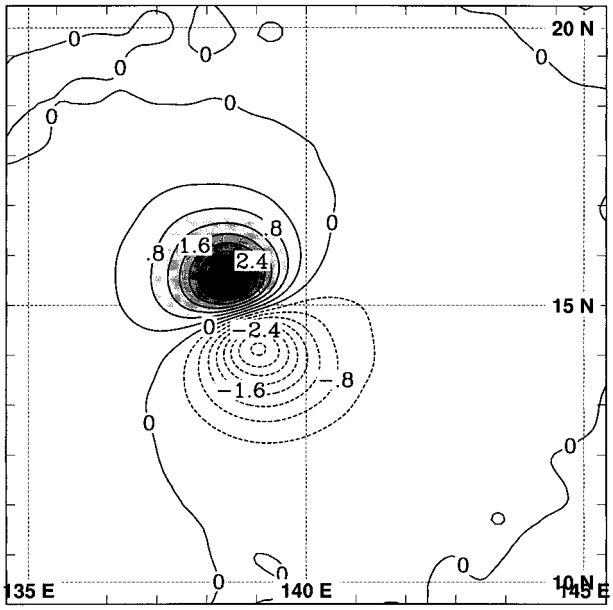

FIG. 7. Vertical velocity (cm s^{-1}) at 500 hPa, 24 h, for case C1. The contour interval is 0.4, and positive values greater than 0.4 are shaded.

almost constant direction. We feel that this difference resulted in part from the use of a baroclinic vortex in the current study, which had decreasing intensity with height, and also from the weaker intensity and larger diameter of the vortex used in the present study.

The secondary circulation described above caused upward displacement of the potential temperature surfaces "down-tilt" from the surface vortex and downward displacement of the isentropes on the opposite side. This produced a cold anomaly west-southwest of the low-level vortex center and a warm anomaly to the east-northeast of the surface low (Fig. 6a). The primary circulation in the low levels (i.e., the main vortex) then produced a wavenumber one asymmetry in the vertical motion field as the strong rotational flow moved along the sloping isentropes. This is illustrated in Fig. 6b, which shows a vertical velocity dipole at 950 hPa with ascending motion in the right front quadrant and descent in the left rear quadrant. Maximum vertical velocities at this time ($t = 24$ h) and level were about ± 0.6 cm s^{-1}. The vertical velocities in Fig. 6b were almost totally due to the isentropic flow, as the ascent along the isentropes was almost two orders of magnitude greater than the diagnosed vertical velocities that were causing the vertical displacement of the isentropes. The pattern extended through most of the troposphere, with the vertical velocities extending upward to between 200 and 300 hPa and reaching maximum values of about ± 3.5 cm s^{-1} in the middle levels (Figs. 7, 8).

In case C2 the boundary layer scheme was activated. Note that in this run the low-level environmental flow was near zero, so the first-order effects of the friction would be expected to be symmetric. The vertical velocities at 24 h at 950 hPa and 500 hPa are shown in Figs. 9 and 10, respectively. At 950 hPa the combined effects of easterly shear and friction in the boundary layer produced asymmetrical low-level convergence that resulted in a vertical velocity pattern that looks roughly like a simple sum of the fields generated by

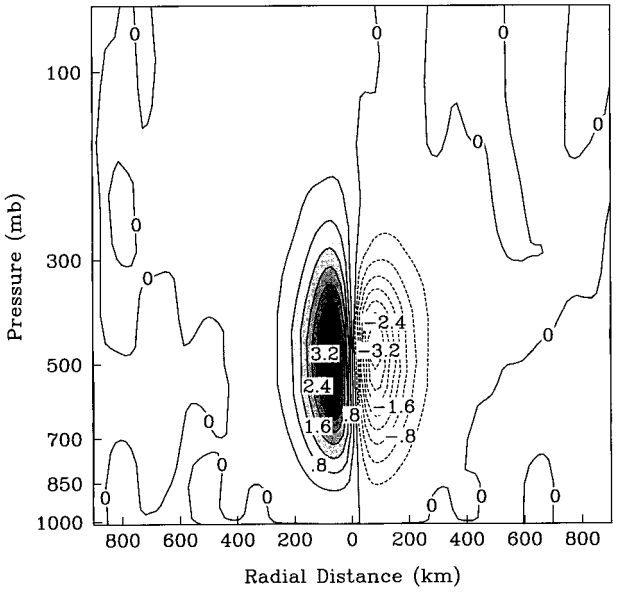

FIG. 8. Vertical cross section of vertical velocity along a northwest–southeast line through the center of the vortex in case C1 at 24 h. The units are cm s^{-1}, the contour interval is 0.4, and positive values greater than 0.4 are shaded.

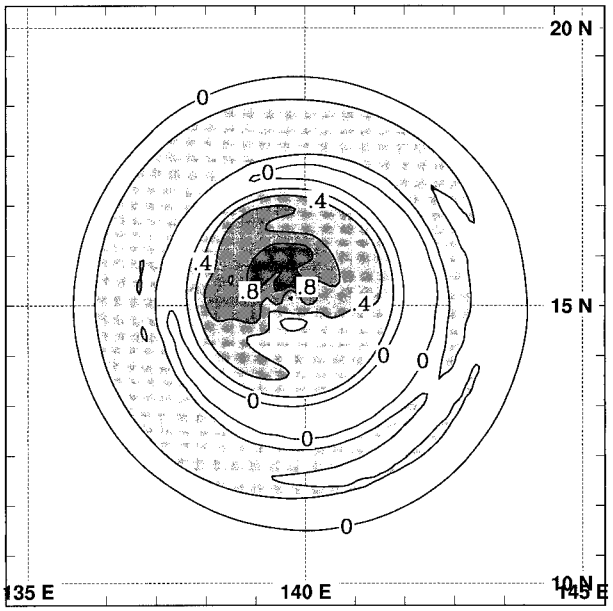

FIG. 9. Vertical velocity (cm s^{-1}) at 950 hPa, 24h, for case C2 (easterly shear, no zonal flow, with boundary layer). The contour interval is 0.2, and positive values greater than 0.2 are shaded.

each process, with banded structure and upward/downward motion in the right front/left rear quadrant. The maximum upward motion in Fig. 9 is 1.0 cm s^{-1}. The vertical motion field at 500 hPa for $t = 24$ h was very similar to that for case C1, showing that the frictional effects were shallow in the core region. (The maximum upward motion at 500 hPa in C2 was about 3.0 cm s^{-1}, slightly less than the 3.4 cm s^{-1} of C1.)

Case C3 was similar to C2, except that with the added low-level storm motion, there was increased asymmetry of the frictional effects upon the divergence field. After 24 h there were two bands of concentrated low-level upward motion at 950 hPa in front of and on the right side of the vortex, with subsidence concentrated on the left side close to the center and to the left and rear at larger radii (Fig. 11). Interestingly, the maximum vertical velocity at this level was 2 cm s^{-1}, stronger than in any of the other cases. Therefore, the combined effects of friction acting on the moving vortex and easterly shear increased the magnitude of the forced uplifting in the right front quadrant. At 500 hPa the vertical velocity pattern had the same dipole structure as for the frictionless case (C1), with the rising motion occurring in the right front quadrant (not shown).

Finally, case C2 was rerun twice with the vertical shear profile shifted such that the maximum shear level occurred near 700 hPa and 350 hPa, respectively. With the shear shifted to lower levels, the storm behaved almost exactly as shown in the above figures for case C2, though the maximum values of the induced vertical velocity field were about 10% stronger. When the shear was shifted to higher levels, the effects on the low-level storm structure were greatly reduced. In terms of modulating the secondary circulation of a tropical cyclone, low-level and midlevel shear appear to be much more important than is upper-level shear.

4) WESTERLY SHEAR CASE: CASE D

The final dry case (D3) had westerly shear, exactly opposite in sign to that shown in Fig. 4, and an easterly

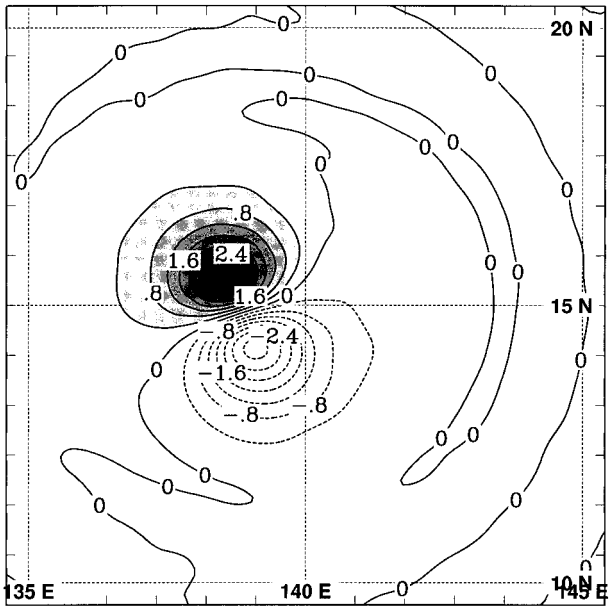

FIG. 10. Vertical velocity (cm s^{-1}) at 500 hPa, 24h, case C2. The contour interval 0.4, and values greater than 0.4 are shaded.

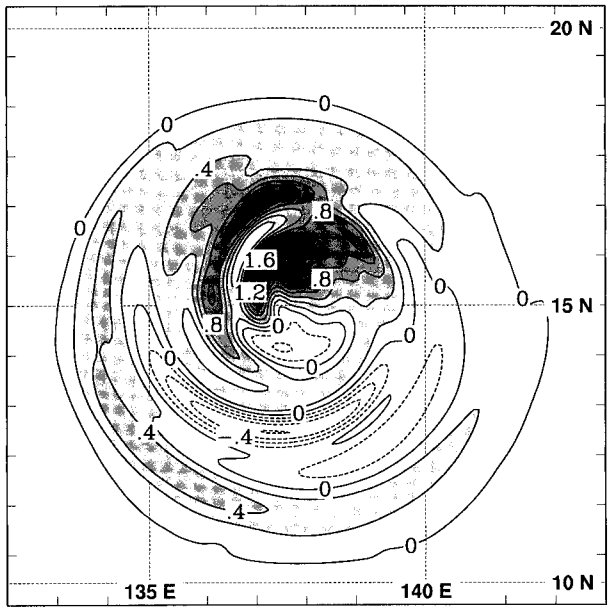

FIG. 11. Vertical velocity (cm s^{-1}) at 950 hPa, 24h, case C3 (easterly zonal flow, easterly shear). The contour interval is 0.2, and values greater than 0.2 are shaded.

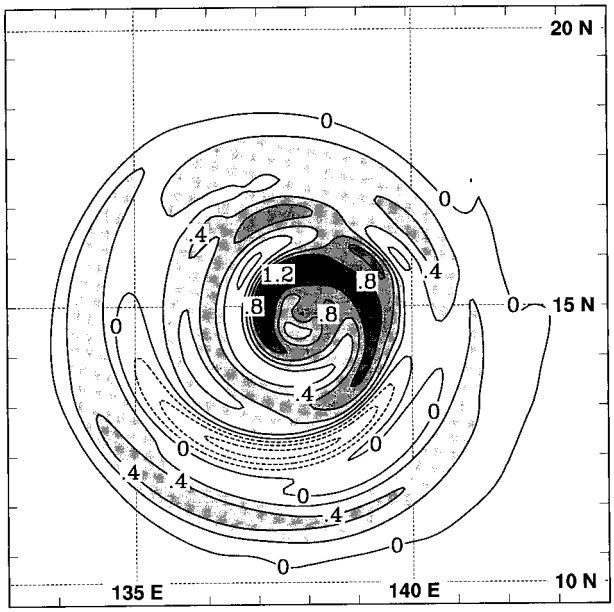

FIG. 12. As in Fig. 11, but for case D3 (easterly zonal flow, westerly shear).

background flow of 3 m s^{-1} was added to the shear. The boundary layer scheme was active. The vertical velocities at $t = 24$ h for the 950-hPa level are shown in Fig. 12. At this level the storm formed a pattern of spiral bands, with the maximum upward motion occurring ahead and slightly to the right of the storm, but the region of upward motion was much more symmetric than in the easterly shear case. The increased symmetry reflects the fact that for this case the low-level convergence areas induced by shear and by friction occur on opposite sides of the center. The maximum vertical velocity in Fig. 12 is 1.2 cm s^{-1}, weaker than the maximum from case C3. At 500 hPa the w pattern was almost exactly a mirror image of case C3, with ascent in the left rear quadrant and descent in the right front quadrant looking downshear (not shown). As in the other shear runs, the vertical velocity field in the middle levels and above resulted almost entirely from the effects of shear rather than from friction.

5) SUMMARY OF DRY SIMULATIONS

Frictional effects tended to focus convergence in a band surrounding the vortex center. When the low-level vortex center moved due to advection by the mean flow, the convergence became asymmetrical and was organized into spiral bands with maximum uplifting ahead of the moving storm center. The boundary layer processes had little effect on the dry vortex above about 850 hPa, but since low-level convergence can play a major role in organizing deep convection and hence latent heat release, these processes could be significant in modulating cyclone structure.

Vertical wind shear caused a three-stage sequence of events. First, the shear tilted the vortex generally downshear, and the lower and upper vortex centers tended to migrate with components to the right/left of the mean shear vector (producing a slight cyclonic rotation of the tilt from directly downshear). The direction of tilt remained almost constant throughout the dry runs. Second, the tilting rapidly unbalanced the vortices creating weak ascent downshear and descent upshear of the low-level vortex center. This initial secondary circulation pattern caused upward/downward bulging of the cold/warm isentropes downshear/upshear of the surface vortex. Third, as this pattern developed, the primary vortex circulation flowed up and down the tilted isentropes producing a vertical circulation pattern with maximum upward motion in the downshear right quadrant (looking downshear) and subsidence in the upshear left quadrant. This shear-induced vertical velocity dipole was quite deep, extending upward to well above 300 hPa in the current study. In these dry simulations the vertical motion was dominated by the final mechanism, that is, the isentropic flow of the primary circulation. Low-level and midlevel shear were found to have much stronger effects on the secondary circulation than upper-level shear for shears of similar magnitude.

The secondary circulation patterns induced by the relatively modest environmental perturbations shown in this study are quite striking, and they strongly suggest shear can modulate the pattern, and perhaps amount, of latent heat release in the core region. Friction plays a more complex role in tropical cyclone structure, but it too appears to be capable of affecting the distribution

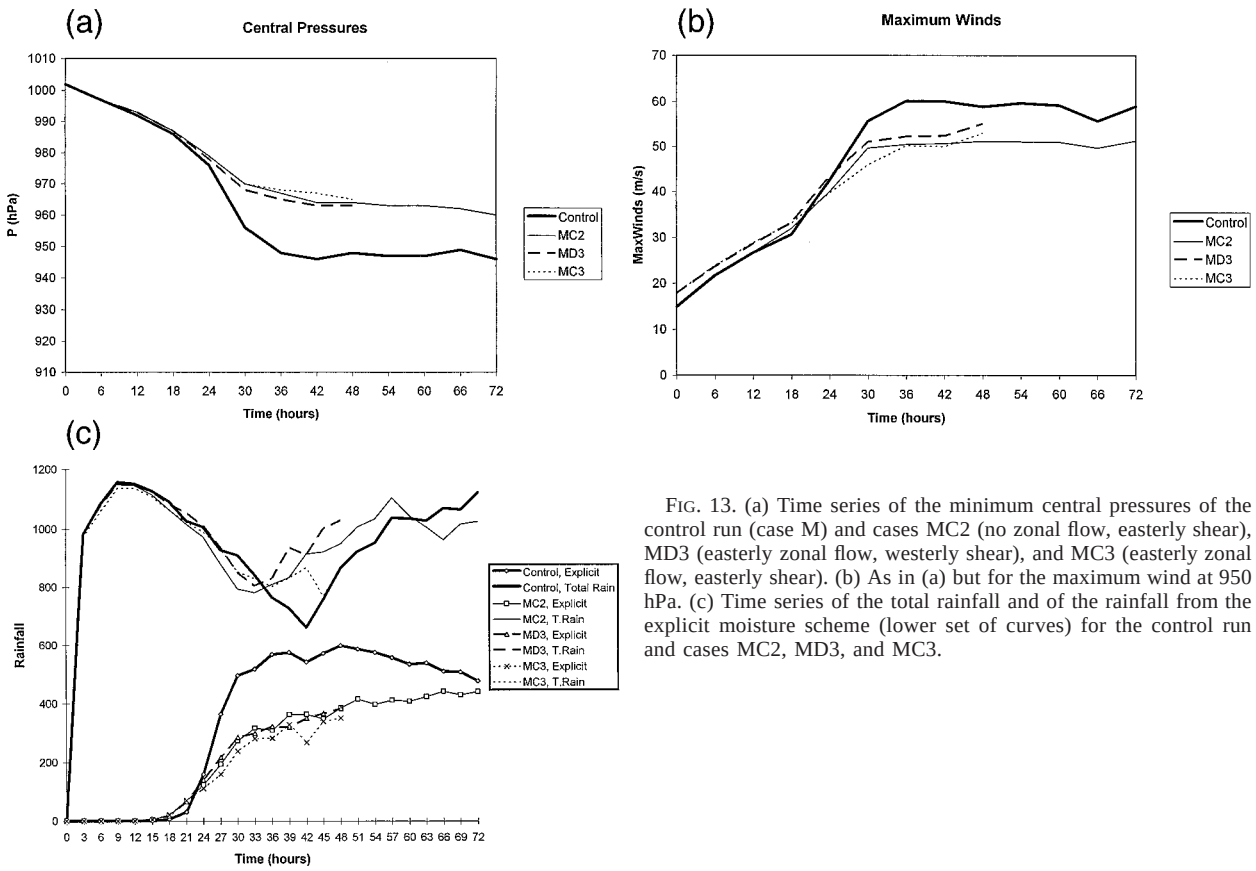

FIG. 13. (a) Time series of the minimum central pressures of the control run (case M) and cases MC2 (no zonal flow, easterly shear), MD3 (easterly zonal flow, westerly shear), and MC3 (easterly zonal flow, easterly shear). (b) As in (a) but for the maximum wind at 950 hPa. (c) Time series of the total rainfall and of the rainfall from the explicit moisture scheme (lower set of curves) for the control run and cases MC2, MD3, and MC3.

of latent heating. This is explored below using the full-physics version of the model.

b. Moist simulations

1) INTENSITY AND MEAN RAINFALL VARIATIONS

Addition of latent heating processes causes profound changes in the evolution of the simulated tropical cyclone, as expected. A control simulation was performed with the same initial conditions as used in the dry runs but with no mean zonal flow (case M). This was followed by four other moist simulations that included sheared zonal flow (Table 1). Case MC2 had the same easterly shear and no added zonal flow as dry case C2. Case MC3 had the easterly shear plus added easterly mean flow used in case C3. Case MD3 had the same westerly shear and easterly zonal flow as dry case D3, and case MD2 had westerly zonal shear but no additional zonal flow.

The control simulation resulted in rapid intensification of the initial vortex into a hurricane. The evolution of the central pressure and rainfall for each of the moist runs can be seen in Fig. 13. The control run reached an approximate steady state at about 36 h with winds of about 60 m s^{-1} and a central pressure that subsequently remained between 946 and 948 hPa. As expected, the storm maintained a symmetric structure throughout the simulation. For the 28.5°C SST used in these runs DeMaria and Kaplan's (1994) data would indicate a maximum potential intensity of around 920 hPa. Given the relatively coarse resolution of the fine mesh (15 km), the control central pressure appears to be reasonable. Based on similarly configured runs being performed locally by colleagues, we would expect the simulation to eventually approach the approximate intensity predicted by DeMaria and Kaplan if it were to continue for several more days (J. L. Evans and S. K. Drury 1998, personal communication).

The rainfall in all of the runs rapidly builds up to a maximum at about $t = 9$ h (Fig. 13). The control run total rainfall then decreases to a minimum value, which occurs near 42 h, and then increases again. The three sheared runs follow similar patterns but experience smaller decreases in total rainfall and reach their minima earlier. The lower set of curves in Fig. 13 show the explicit rainfall for each run, and the parameterized rainfall is equal to the difference between the curves. For the first 15–18 h virtually all rainfall is convective (parameterized) in all of the runs. Beginning around 18 h the explicit rainfall begins to grow, and it is of the order of half of the total rainfall in the sheared runs from about 36 h onward. In the control run, however, the

explicit rainfall grows faster and represents a much larger fraction of the total rainfall. The rainfall shown is averaged over the fine mesh area, but most of the rain falls within 300 km of the storm center. Explicit rain is concentrated primarily within and immediately adjacent to the eyewall cloud. The control run develops a more compact structure with a greater fraction of its overall rainfall occurring in the eyewall than do any of the shear runs.

All of the simulations exhibit rather stable intensities from 30 h onward despite relatively large changes in total rainfall. However, the explicit rainfall, which is concentrated in the storm cores, is much steadier than the parameterized rainfall during this period. The data in Fig. 13 suggest that the storm intensity is closely related to the rainfall in the eyewall but not to variations in the convective rainfall at greater radii.

2) EVOLUTION OF STORM STRUCTURE

Cases MC2 and MD2 (easterly/westerly shear, no additional zonal flow) produced identical results except that the patterns are rotated 180° from each other. This is expected for the initial conditions used since the simulations are on an f-plane. We present results only for the MC2 run here, but the results for MD2 can be visualized by rotating the MC2 results. Case MC2 intensified and developed into a hurricane, reaching an approximate steady-state intensity near 36 h (Fig. 13). The mature storm reached a central pressure of about 963 hPa and maximum winds of about 51 m s^{-1}. Only slight fluctuations in these values occurred throughout the remainder of the 72-h simulation. The mature MC2 storm was weaker than the control run storm by about 15 hPa and 5–10 m s^{-1}.

Due to the lack of large-scale winds in the lower levels, the MC2 storm moved very slowly, drifting slightly to the northwest under the influence of the shear. Low-level convergence rapidly produced nearly symmetric uplifting and rainfall in run MC2. However, within a few hours the storm developed a significant asymmetry in the vertical velocity field, with the maximum uplifting occurring due west of the storm center (directly downshear). This appeared to result initially from the same process that caused vertical velocity in the very early stages of dry case C2. That is, the shear begins to tilt the vortex downshear due to increasing vorticity advection with height. The downward projection of the midlevel PV anomaly causes convergence in the low levels and uplifting through the lower and middle troposphere directly west/downshear of the surface center. Midlevel convergence, low-level divergence, and subsidence are induced east (upshear) of the surface center by this process. The modulation of the vertical velocity field causes a similar modulation of the convection (not shown).

From 6 to 12 h, MC2 continued to behave somewhat like run C2 but with convection greatly amplifying the vertical velocity field. A cold anomaly developed at 700 hPa west (downshear) of the storm, and for a while there was maximum upward motion at this level in the northwest (downshear right) quadrant where the isentropic uplifting of the primary flow was strongest (Figs. 14, 6). However, between 18 and 24 h the flow in the eyewall became saturated at many grid points, and the combined effects of the explicit and parameterized latent heat release destroyed the cold anomaly and hence the isentropic uplifting mechanism. The maximum uplifting and rainfall tended to become collocated with the warmest temperatures, southwest of the center. After 24 h, the vertical velocity field of MC2 at 950 hPa indicates that the convection in the eyewall had become somewhat cellular but was strongest in the southwest quadrant (Fig. 15).

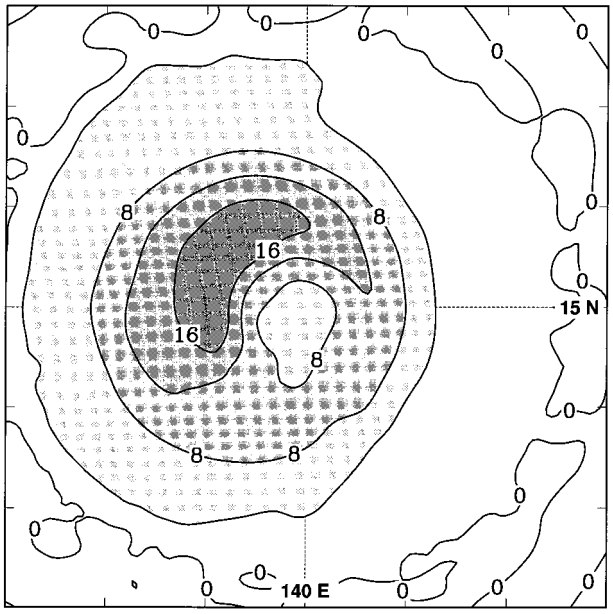

FIG. 14. Vertical velocity (cm s^{-1}) at 950 hPa, $t = 12$ h, case MC2 (easterly shear, no zonal flow). The contour interval is 4.0, and values greater than 4.0 are shaded. The area shown is 600 km square.

Figures 16a–c show the 700-hPa vertical velocity, cloud water, and rainwater at 48 h, when the storm structure was mature and relatively steady. (The 700-hPa level was chosen for display since vertical motion at this level has a strong correlation with net latent heat release.) Note that the rainwater pattern was slightly cyclonically rotated from the maximum upward motion and cloud water due to advection of the rainwater. This is generally true throughout the moist runs. The cloud water was coincident with the upward motion. Throughout most of the 72 h of this run the strongest rainfall occurred to the downshear left (southwest) of the storm center. The strongest winds tended to occur in the southeast quadrant of the storm (upshear left, looking downshear), and there was also a weak local maximum due east of the center at 48 h (Fig. 17). Summarizing, the

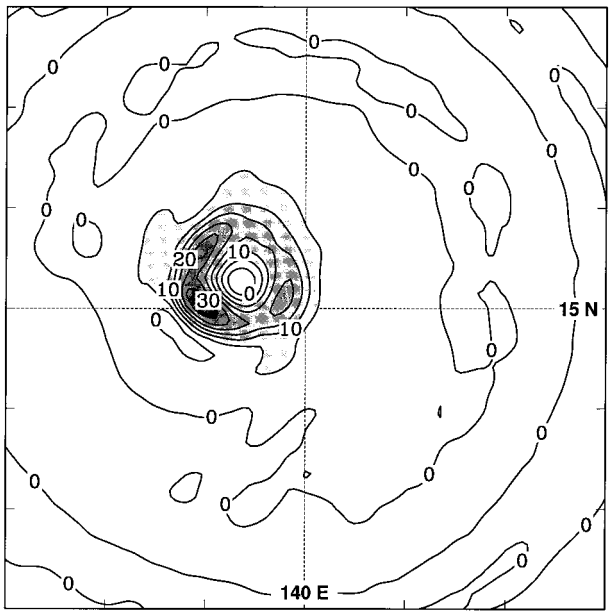

FIG. 15. As in Fig. 14, but at $t = 24$ h. The contour interval is 5.0, and values greater than 5.0 are shaded.

addition of moist processes resulted in a shift of the maximum convection from the downshear right quadrant predicted from the adiabatic simulation, to the downshear left quadrant. This was primarily because the isentropic lifting mechanism that dominated the dry runs was removed when the eyewall became saturated allowing the first-order vorticity advection effects to dominate the vertical motion field instead.

When easterly zonal flow was added to the easterly shear background (MC3), the storm moved on a track that was just slightly north of westerly and evolved through a life cycle pattern that closely resembled that of MC2 with respect to patterns of growth and intensity change. In the dry version of this case (C3), the adiabatic uplifting mechanism and frictional convergence in the boundary layer both tended to produce forced uplifting in the downshear-right quadrant, northwest of the westward-moving storm. Hence, C3 was the most asymmetrical of the dry runs. However, this did not hold true for the moist version. Once the storm in MC3 approached maturity and developed a saturated eyewall cloud, the region of maximum vertical motion and latent heat release tended to shift to the downshear-left quadrant, south of the westward-moving storm center. However, by 48 h, the low-level, upward motion in the eyewall was relatively evenly distributed around the center (Fig. 18), with the maximum value occurring in the front right quadrant of the storm center, consistent with frictional forcing asymmetries for a westward-moving storm. The cloud water and rainwater for this run at 700 hPa and 48 h (Fig. 19) were typical of the mature stage of the simulation. They show the tendency for upward motion and rainfall to be concentrated in the eyewall cloud ranging from north of the center counterclockwise through south to southeast of the center. The eyewall was open, or clear, to the northeast (upshear right), and maximum winds were located in the northeast quadrant, which for this case was both the right back quadrant relative to motion and the upshear right quadrant relative to the shear vector (Fig. 20).

When the zonal flow remained easterly, but the direction of the background shear was changed from easterly to westerly (MD3), the storm evolved through a life cycle pattern that resembled those of MC2 and MC3. In the dry version of this case (D3), the adiabatic uplifting mechanism produced forced uplifting in the downshear right quadrant (southeast), whereas frictional convergence in the boundary layer tended to produce forced uplifting in the front right quadrant (northwest) of the westward-moving storm. Hence, D3 was the most symmetrical of the dry runs. When moist physics were included, the storm motion produced frictional convergence in the boundary layer to the west and northwest of the center similar to that discussed for MC3. By 48 h the vertical velocity at 950 hPa showed maximum uplifting in the eyewall concentrated in a band that ran clockwise from west (in the direction of motion) through northeast (downshear left) of the storm center (Fig. 21). The vertical velocity at 700 hPa at this time was even more asymmetrical and showed the effects of convection concentrated in two regions, west and northeast of the center (not shown). The cloud water and rainwater at 700 hPa showed an open or clear region of the eye to the south-southeast, with maximum values generally west and north of the center (Fig. 22). Maximum winds were located in the northwest quadrant, which for this case was both the right front quadrant relative to motion and the upshear left quadrant relative to the shear vector (Fig. 23). The patterns throughout the 48 h of the simulation tended to resemble those of MC3, though rotated between 90° and 180° in the counterclockwise direction. However, the difference in direction between the zonal flow and shear vector in case MD3 resulted in a second area of preferred convection forced by asymmetries in the boundary layer friction. The convection in this region located west to northwest of the center was comparable in magnitude to that in the region forced by the westerly shear (downshear left or northeast of the center).

In both MC3 and MD3 the frictional convergence and the shear tended to force ascent in different sectors of their eyewall clouds. There were differences in the relative locations of the two modes, with the shear-induced uplifting occurring upstream of the frictional convergence area in MD3 and downstream in MC3. (Upstream in this instance refers to the rotational flow in the eyewall region, not the storm motion vector.) However, the two runs contained about the same degree of wavenumber one asymmetry, and their intensities were only slightly different.

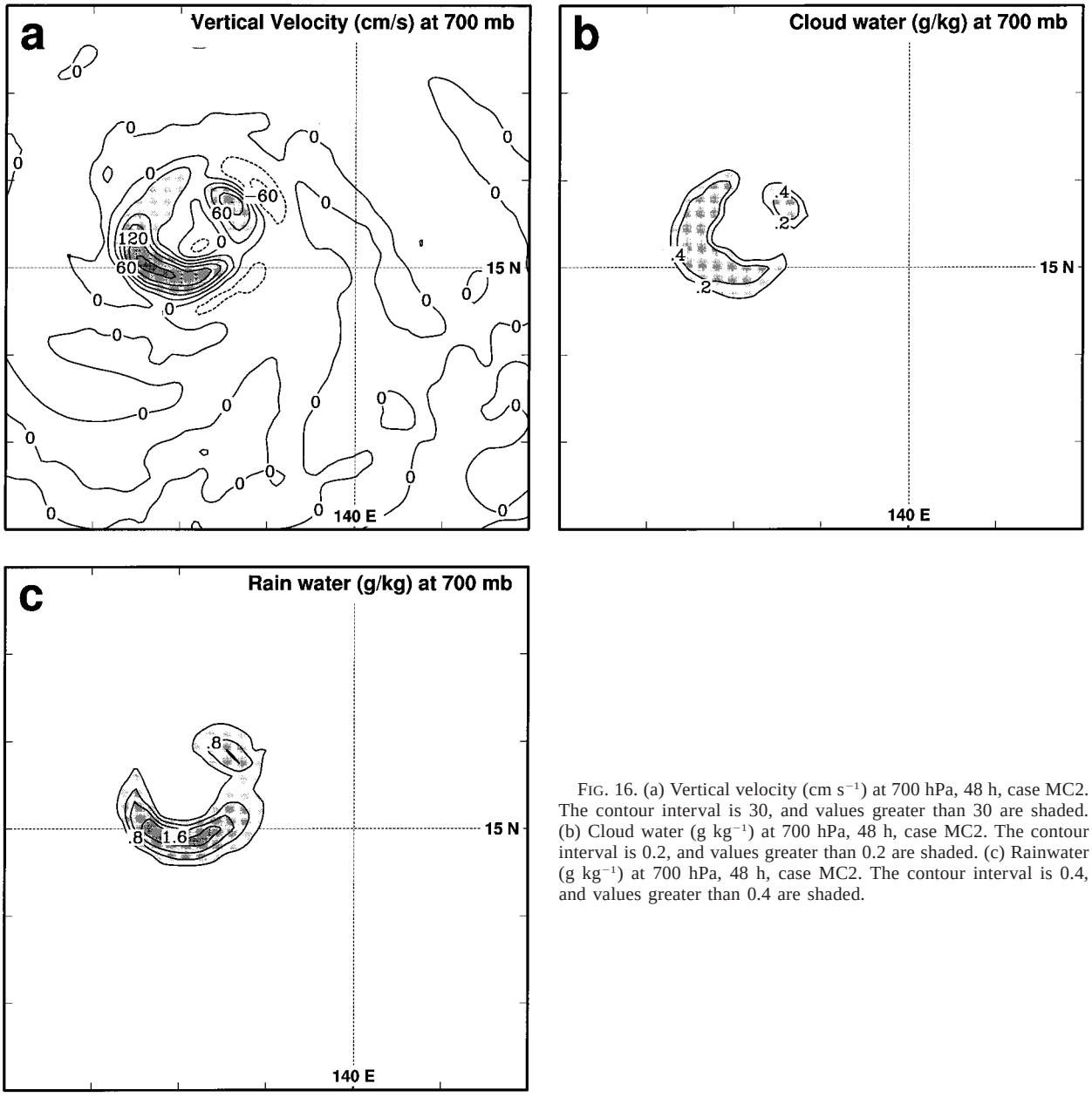

FIG. 16. (a) Vertical velocity (cm s^{-1}) at 700 hPa, 48 h, case MC2. The contour interval is 30, and values greater than 30 are shaded. (b) Cloud water (g kg^{-1}) at 700 hPa, 48 h, case MC2. The contour interval is 0.2, and values greater than 0.2 are shaded. (c) Rainwater (g kg^{-1}) at 700 hPa, 48 h, case MC2. The contour interval is 0.4, and values greater than 0.4 are shaded.

An interesting facet of runs MC2, MC3, and MD3 is that once each storm became mature, it tended to develop asymmetries in the eyewall. The predominant pattern was usually a wavenumber one asymmetry. However, at various times the eyewall structure developed asymmetries that appeared to have wavenumber 2 structure, and occasionally it appeared as if the overall structure exhibited wavenumber 4 features. It is difficult to distinguish whether apparent higher-order modes were due to vortex-scale dynamics or reflected localized growth of convective cells, but the persistence of the patterns observed in the eyewall structure suggests the presence of wavenumber four asymmetries during days 2 and 3. We did not explore this further in the current paper, but will do so in future studies. The occurrence of asymmetries in the eyewall flow and the dominance of the wavenumber one pattern are in qualitative agreement with the studies of vortex Rossby waves by Montgomery and Kallenbach (1997).

4. Conclusions and recommendations

The dry simulations showed that both storm motion and weak vertical shear produce wavenumber one asymmetries in the low-level convergence field. For the friction, the area of forced ascent is ahead and to the right

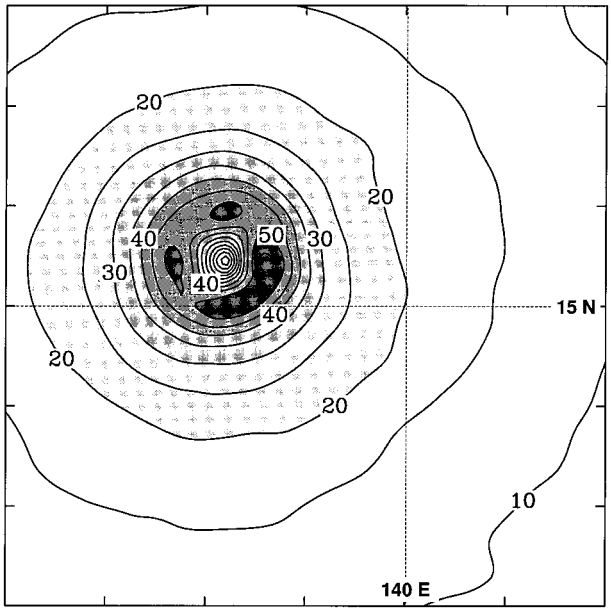

FIG. 17. Wind speed (m s^{-1}) at 950 hPa, 48 h, case MC2. Contour interval is 5 m s^{-1}.

of the storm track for the values tested here, and this agrees with the results of Shapiro (1983). The shear-induced ascent extends through a much deeper layer and tends to be concentrated in the quadrant downshear right of the storm center. This pattern results from a three-stage process. The shear causes increasing advection of PV with height, and this forces a weak secondary circulation with ascent downshear and descent upshear of

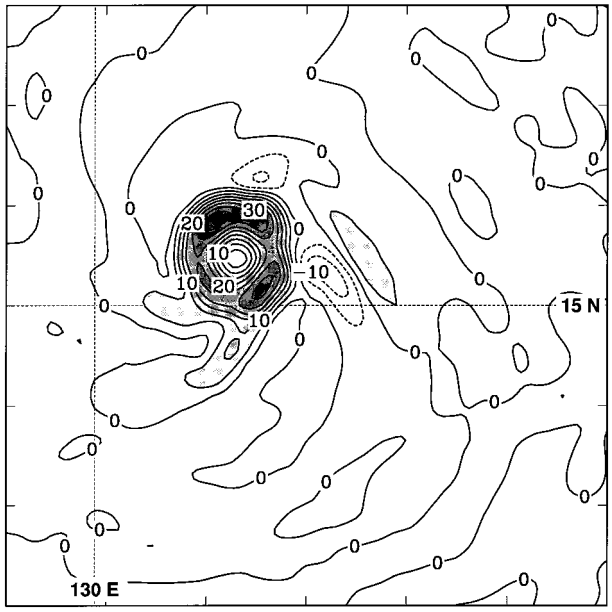

FIG. 18. Vertical velocity (cm s^{-1}) at 950 hPa, 48 h, case MC3 (easterly zonal flow, easterly shear). The contour interval is 5.0, and values greater than 5.0 are shaded.

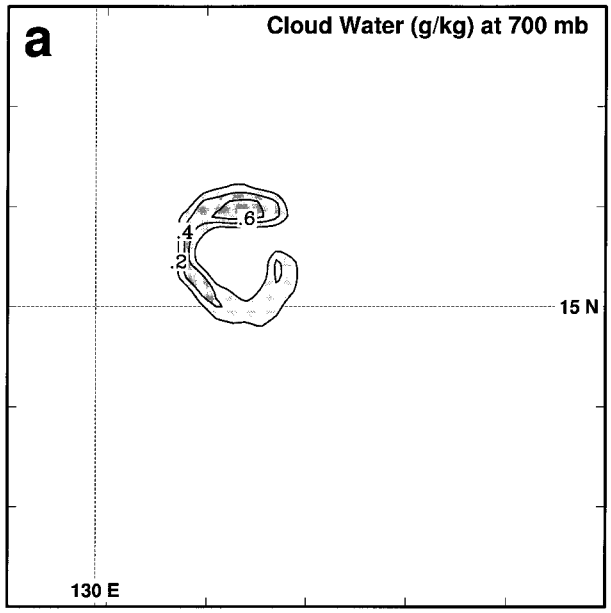

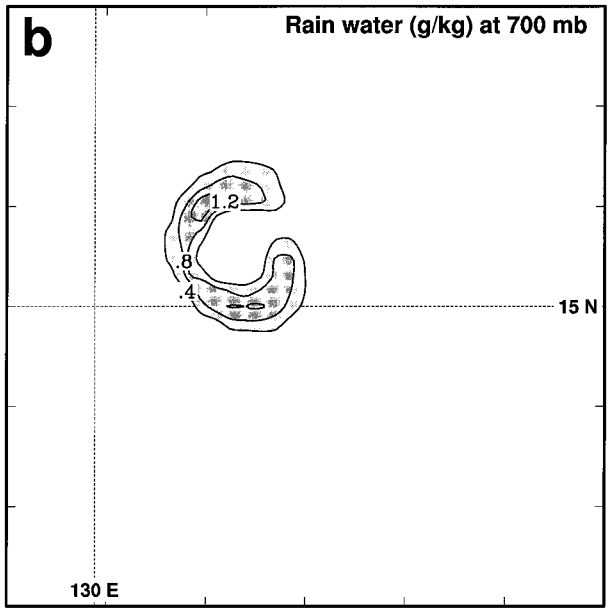

FIG. 19. (a) Cloud water (g kg^{-1}) at 700 hPa, 48 h, case MC3. The contour interval is 0.2. (b) Rainwater (g kg^{-1}) at 700 hPa, 48 h, case MC3. The contour interval is 0.4.

the surface vortex center. The vertical distortion of the isentropes resulting from this circulation causes the primary rotational flow of the vortex to ascend and descend isentropically. The mechanism dominating the shear-induced vertical motion pattern in the dry runs is the latter isentropic lifting mechanism, which was described by Jones (1995). Low-level and midlevel shear have much stronger effects on the vertical motion field than does upper-level shear.

All of the moist runs stabilized in a quasi-mature state

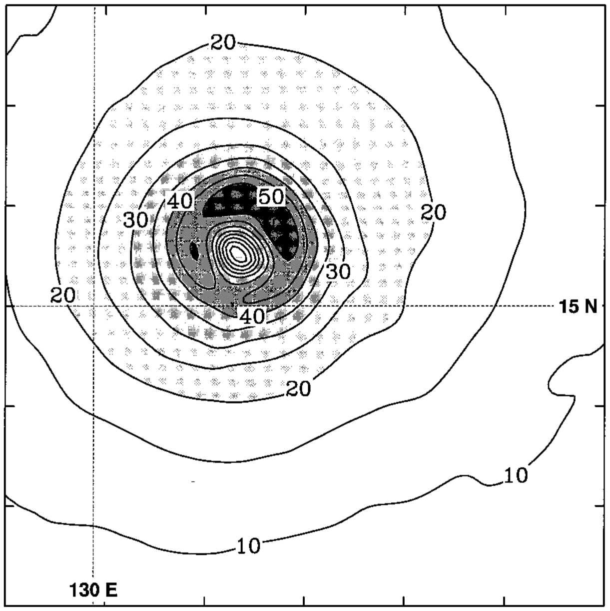

FIG. 20. Wind speed (m s^{-1}) at 950 hPa, 48 h, case MC3. The contour interval is 5.0.

after about 30 h, and the runs in sheared flow exhibited central pressures that were markedly higher than those in the control run. The control run did not develop more total rainfall than the sheared storms, but it did have more explicit rainfall concentrated in the eyewall region. Each storm in sheared flow developed significant asymmetries in the azimuthal distribution of winds and rain within the eyewall region.

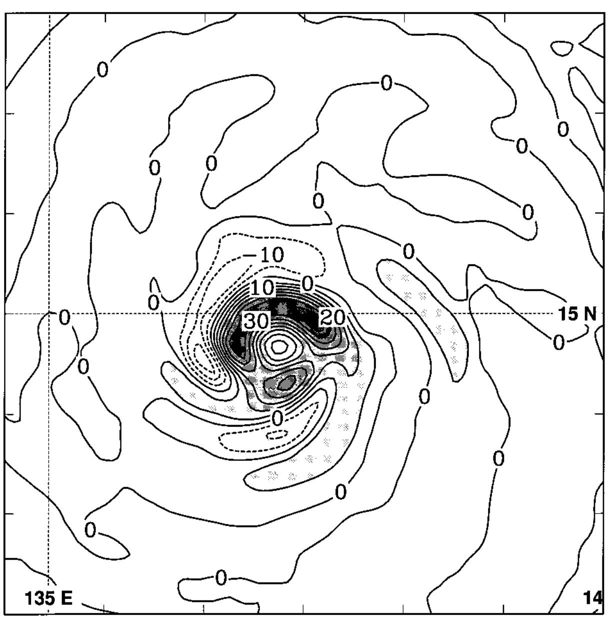

FIG. 21. Vertical velocity (cm s^{-1}) at 950 hPa, 48 h, case MD3 (easterly zonal flow, westerly shear). The contour interval is 5.0, and values greater than 5.0 are shaded.

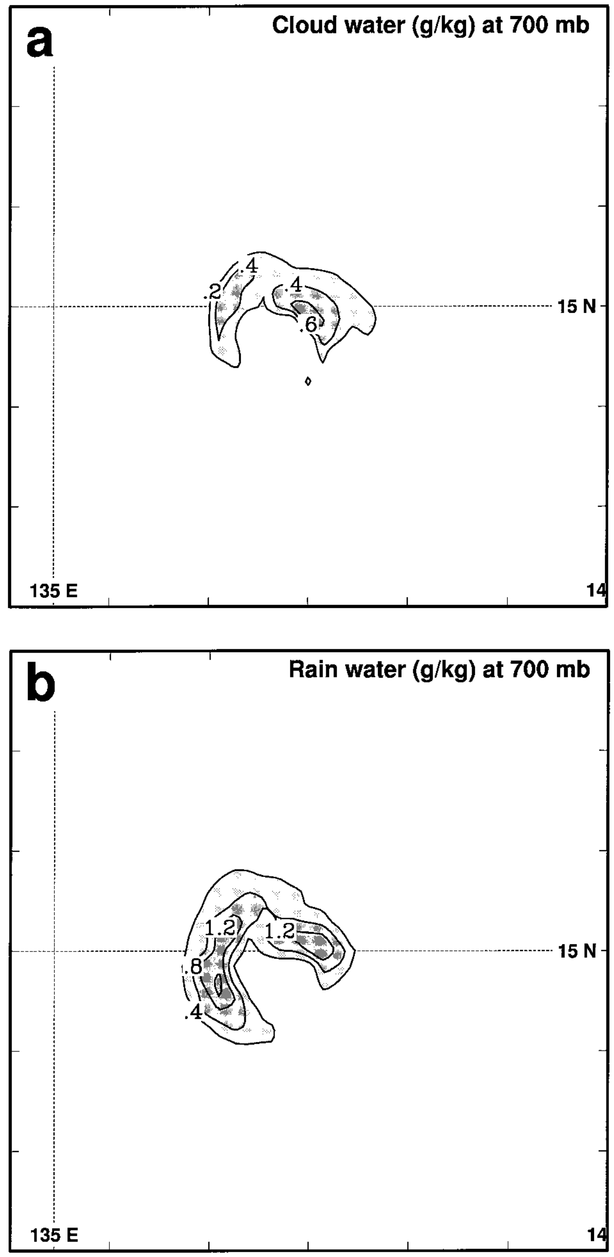

FIG. 22. (a) Cloud water (g kg^{-1}) at 700 hPa, 48 h, case MD3. The contour interval is 0.2. (b) Rainwater (g kg^{-1}) at 700 hPa, 48 h, case MD3. The contour interval is 0.4.

It was hypothesized that strong asymmetric forcing of upward vertical velocity in the core of the simulated hurricanes would produce marked asymmetries in the patterns of latent heat release in the core structure, and that this would affect the storm's intensity. This proved to be the case, but the results show that the effects of the latent heat release alter the pattern of convection once the storm approaches a mature structure.

The asymmetry in boundary layer convergence showed the same relationship with storm motion in the

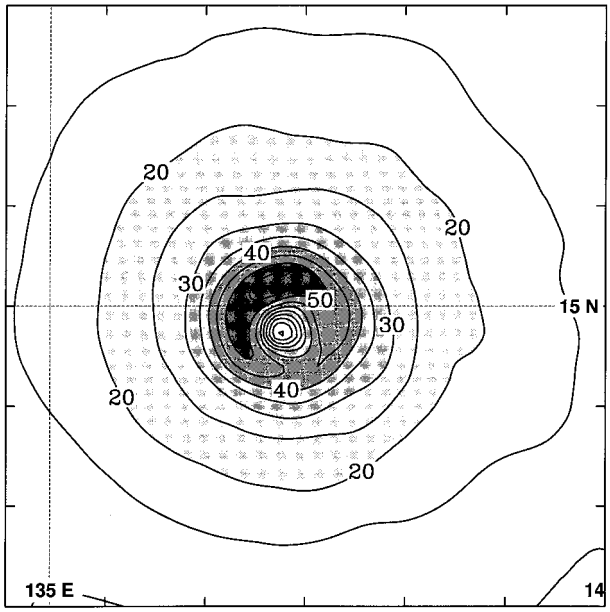

FIG. 23. Wind speed (m s^{-1}) at 950 hPa, 48 h, case MD3. The contour interval is 5.0.

dry and moist runs, with the maximum convergence occurring ahead and to the right of the storm motion vector in the two cases that exhibited significant storm motion. However, the vertical shear tended to produce maximum convection to the left of the shear vector, looking downshear, once the storms developed saturated regions within their eyewalls. The upward motion and convection were then concentrated in the downshear left quadrant, while the rainwater was advected around to the left of the shear. The reason for the differences in shear effects between dry and moist runs is that once resolvable latent heat release is established in the eyewall, the diabatic heating destroys the adiabatic lifting mechanism that dominates the vertical velocity patterns in the dry runs. In the moist runs the secondary circulation component forced by vertical shear is due to the direct effects of differential vorticity advection upon a quasi-balanced vortex.

The simulated rainfall patterns associated with vertical shear agree with radar observations of hurricane cores (Willoughby 1984; H. E. Willoughby 1998, personal communication; Marks et al. 1992; Franklin et al. 1993), and with the easterly shear case simulated by Bender (1997). Since both storm motion and large-scale shear can be predicted with some accuracy, the results of this study indicate that the structure of the hurricane core and intensity should be predictable as well. The results suggest that the response to shear should be different in loosely organized convective systems, such as tropical depressions that usually lack a saturated eyewall cloud, than they are in mature hurricanes. This will be examined in future work.

The current study examined a limited range of values of zonal flow and unidirectional vertical shear. In the current study the shear and boundary layer friction had approximately equal effects on modulating the latent heat release in the core. However, the values of shear used were relatively weak compared to the shears experienced by many real hurricanes. The storm motions (or order 3 m s^{-1}) were more comparable to typically observed storm speeds (though they were still below average). Even these relatively modest values were able to force the storms to develop major wavenumber one asymmetries, and higher-order wavenumbers were suggested by temporal variations in the eyewall structures. It is hypothesized that these asymmetries in the eyewall structure are responsible for the reduced intensities of the sheared storms relative to the control storm. However, the physical link between asymmetrical structure and storm intensity change is a topic of our ongoing research. Further diagnostics and additional simulations are in progress.

The work shown in this paper represents only one part of the study. In addition, the same model and approach are being used to examine the effects of vortex mergers and of asymmetrical distributions of latent heat release, both in the core and in the rainbands, upon cyclone structure and intensity. The next stage of the research, which will use a finer grid mesh and explicit moist processes to resolve convective processes, is under way and will be reported upon in a subsequent paper. An obvious area for future work is to expand the study through a wider range of parameter space, including the introduction of directional shear and of shear with different orientations relative to the mean flow. We plan to do this, as well as to study the effects of performing the simulations on a β-plane and in regions with variations in SST.

Acknowledgments. This research was supported by the National Science Foundation Division of Atmospheric Sciences through Grant ATM-9523667, and the Office of Naval Research Division of Marine Meteorology through Grant N00014-96-1-0582. The authors also wish to thank the two anonymous reviewers for their helpful comments.

REFERENCES

Anthes, R. A., E.-Y. Hsie, and Y.-H. Kuo, 1987: Description of the PSU/NCAR mesoscale model version 4 (MM4). NCAR Tech. Note NCAR/TN-282+STR, 66 pp.

Bender, M. A., 1997: The effect of relative flow on the asymmetric structure of the interior of hurricanes. *J. Atmos. Sci.,* **54,** 703–724.

Betts, A. K., and M. Miller, 1986: A new convective adjustment scheme. Part II: Single column tests using GATE wave, BOMEX, ATEX and arctic air-mass data sets. *Quart. J. Roy. Meteor. Soc.,* **112,** 693–709.

Blackadar, A. K., 1976: Modeling the nocturnal boundary layer. Preprints, *Third Symp. on Atmospheric Turbulence and Air Quality,* Raleigh, NC, Amer. Meteor. Soc., 46–49.

——, 1979: High resolution models of the planetary boundary layer.

Vol. 1, *Advances in Environmental Science and Engineering*, Gordon and Briech Scientific Publishing, 50–85.
DeMaria, M., 1996: The effect of vertical shear on tropical cyclone intensity change. *J. Atmos. Sci.,* **53,** 2076–2087.
——, and J. Kaplan, 1994: Sea surface temperature and the maximum intensity of Atlantic tropical cyclones. *J. Climate,* **7,** 1324–1334.
Emanuel, K. A., 1986: An air–sea interaction theory for tropical cyclones. Part I: Steady-state maintenance. *J. Atmos. Sci.,* **43,** 585–604.
——, 1988: The maximum intensity of hurricanes. *J. Atmos. Sci.,* **45,** 1143–1155.
——, 1997: Some aspects of hurricane inner-core dynamics. *J. Atmos. Sci.,* **54,** 1014–1026.
Frank, W. M., 1977: The structure and energetics of the tropical cyclone. Part II: Dynamics and energetics. *Mon. Wea. Rev.,* **105,** 1136–1150.
——, 1982: Large scale characteristics of tropical cyclones. *Mon. Wea. Rev.,* **110,** 572–586.
——, 1984: A composite analysis of the core of a mature hurricane. *Mon. Wea. Rev.,* **112,** 2401–2420.
Franklin, J. L., S. J. Lord, S. E. Feuer, and F. D. Marks Jr., 1993: The kinematic structure of Hurricane Gloria (1985) determined from nested analyses of dropwinsonde and Doppler wind data. *Mon. Wea. Rev.,* **121,** 2433–2451.
Gray, W. M., 1968: Global view of the origin of tropical disturbances and storms. *Mon. Wea. Rev.,* **96,** 669–700.
Holland, G. J., 1997: The maximum potential intensity of tropical cyclones. *J. Atmos. Sci.,* **54,** 2519–2541.
Jones, S. C., 1995: The evolution of vortices in vertical shear. Part I: Initially barotropic vortices. *Quart. J. Roy. Meteor. Soc.,* **121,** 821–851.
Lighthill, J., G. Holland, W. Gray, C. Landsea, G. Craig, J. Evans, Y. Kurihara, and C. Guard, 1994: Global climate change and tropical cyclones. *Bull. Amer. Meteor. Soc.,* **75,** 2147–2157.
Marks, F. D., Jr., R. A. Houze Jr., and J. F. Gamache, 1992: Dual-aircraft investigation of the inner core of Hurricane Norbert. Part I: Kinematic structure. *J. Atmos. Sci.,* **49,** 919–942.
McBride, J. L., and R. M. Zehr, 1981: Observational analysis of tropical cyclone formation. Part II: Comparison of non-developing versus developing systems. *J. Atmos. Sci.,* **38,** 1132–1151.
Merrill, R. T., 1988: Environmental influences on hurricane intensification. *J. Atmos. Sci.,* **45,** 1678–1687.
Molinari, J., S. Skubis, and D. Vollaro, 1995: External influences on hurricane intensity. Part III: Potential vorticity structure. *J. Atmos. Sci.,* **52,** 3593–3606.
Montgomery, M. T., and R. J. Kallenbach, 1997: A theory for vortex Rossby waves and its application to spiral bands and intensity changes in hurricanes. *Quart. J. Roy. Meteor. Soc.,* **123,** 535–565.
Moss, M. S., and F. J. Merceret, 1976: A note on several low-layer features of Hurricane Eloise (1975). *Mon. Wea. Rev.,* **104,** 967–971.
Pfeffer, R. L., and M. Challa, 1992: The role of environmental asymmetries in Atlantic hurricane formation. *J. Atmos. Sci.,* **49,** 1051–1059.
Shapiro, L. J., 1983: Asymmetric boundary layer flow under a translating hurricane. *J. Atmos. Sci.,* **40,** 1984–1998.
——, 1992: Hurricane vortex motion and evolution in a three-layer model. *J. Atmos. Sci.,* **49,** 140–153.
——, and H. E. Willoughby, 1982: The response of balanced hurricanes to local sources of heat and momentum. *J. Atmos. Sci.,* **39,** 378–394.
Smith, R. K., 1968: The surface boundary layer of a hurricane. *Tellus,* **20,** 473–484.
Willoughby, H. E., 1995: Mature structure and evolution. *Global Perspectives on Tropical Cyclones,* World Meteorological Organization Rep. TCP-38, 21–62.
——, F. D. Marks Jr., and R. J. Feinberg, 1984: Stationary and moving concentric bands in hurricanes. *J. Atmos. Sci.,* **41,** 3189–3211.
Zhang, D.-L., and R. A. Anthes, 1982: A high-resolution model of the planetary boundary layer—Sensitivity tests and comparisons with SESAME-79 data. *J. Appl. Meteor.,* **21,** 1594–1609.